BIOCHEMISTRY
including biophysical chemistry & molecular biology

Article

pubs.acs.org/biochemistry

Nanomechanical Property Maps of Breast Cancer Cells As Determined by Multiharmonic Atomic Force Microscopy Reveal Syk-Dependent Changes in Microtubule Stability Mediated by MAP1B

Mariya O. Krisenko,[†,§] Alexander Cartagena,[‡,∥] Arvind Raman,*[,‡,∥] and Robert L. Geahlen*[,†,§]

[†]Department of Medicinal Chemistry and Molecular Pharmacology, [‡]School of Mechanical Engineering, [§]Purdue Center for Cancer Research, and [∥]Birck Nanotechnology Center, Purdue University, West Lafayette, Indiana 47907, United States

Supporting Information

ABSTRACT: The Syk protein-tyrosine kinase, a well-characterized modulator of immune recognition receptor signaling, also plays important, but poorly characterized, roles in tumor progression, acting as an inhibitor of cellular motility and metastasis in highly invasive cancer cells. Multiharmonic atomic force microscopy (AFM) was used to map nanomechanical properties of live MDA-MB-231 breast cancer cells either lacking or expressing Syk. The expression of Syk dramatically altered the cellular topography, reduced cell height, increased elasticity, increased viscosity, and allowed visualization of a more substantial microtubule network. The microtubules of Syk-expressing cells were more stable to nocodazole-induced depolymerization and were more highly acetylated than those of Syk-deficient cells. Silencing of MAP1B, a major substrate for Syk in MDA-MB-231 cells, attenuated Syk-dependent microtubule stability and reversed much of the effect of Syk on cellular topography, stiffness, and viscosity. This study illustrates the use of multiharmonic AFM both to quantitatively map the local nanomechanical properties of living cells and to identify the underlying mechanisms by which these properties are modulated by signal transduction machinery.

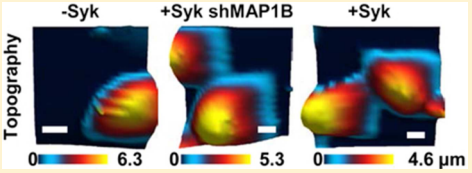

Recent advances in the use of atomic force microscopy (AFM) to record nanomechanical properties of live cells in liquid media make it possible to map quantitatively heterogeneous differences in cellular topography, elasticity, and viscosity at high resolution.[1] For example, local property maps of rat fibroblasts using multiharmonic AFM are sufficiently detailed for visualization of components and properties of the actin cytoskeleton.[1] Unlike conventional quasi-static techniques in which the bending of the cantilever probe is monitored as a function of indentation into the cell at each pixel, multiharmonic AFM is a dynamic AFM method in which the cantilever probe is excited by Lorentz forces and changes in amplitude, the phase of the oscillator, and other relevant harmonics are converted into quantitative local property maps.[1] This mode works in the amplitude modulation (AM-AFM) scheme in which the oscillation amplitude is regulated as the probe scans over the cell. Changes in the physical properties of cells caused by rearrangements in cytoskeletal networks underlie the ability of cancer cells to progress from a static phenotype to a metastatic phenotype.[2] This process is, in turn, controlled by signaling cascades regulated through multiple effectors,[3,4] including the protein-tyrosine kinase Syk,[5,6] but the mechanisms involved are poorly understood. In this study, we examined the utility of multiharmonic AFM for the characterization of Syk-dependent changes in the physical properties of cancer cells as a method of both quantifying physical differences in cells expressing or lacking the kinase and identifying the underlying mechanisms.

Syk is a 72 kDa protein-tyrosine kinase and well-characterized component of the apparatus required for transducing signals initiated by the activation of immune recognition receptors in the innate and adaptive immune systems.[7,8] While a critical role for Syk in immune cell function is clear, a less familiar role in the progression of cancer cells of nonhematopoietic origins has become evident. Syk has been described both as a tumor promoter on the basis of its pro-survival functions in Ras-transformed pancreatic and lung cancer cells[5] and retinoblastoma[9] and as a tumor suppressor on the basis of its loss from many highly invasive tumor cells.[10−17] For example, while Syk is present in relatively nonaggressive breast cancer cells and cell lines, it is absent from cancer cells with a highly invasive, metastatic phenotype.[10] Reintroduction of the kinase into malignant breast carcinomas inhibits their motility, invasion, and metastasis.[10,18] Similarly, the loss of Syk from relatively noninvasive breast epithelial cells decreases the number of cell−cell junctions, enhances cell motility and invasion, and promotes the conversion of cells from an epithelial phenotype to a mesenchymal phenotype.[6,18] Changes in the mechanical properties of tumor cells that accompany an epithelial to mesenchymal transition (EMT) require rearrangements in their cytoskeletal networks, involving both microtubules and microfilaments.[2,19,20] In general, cells move through an extension of lamellipodia at the front of the cell driven primarily by actin polymerization[21] and retraction of the

Special Issue: New Frontiers in Kinases

Received: March 15, 2014
Revised: May 28, 2014
Published: June 10, 2014

   dx.doi.org/10.1021/bi500325n | *Biochemistry* 2015, 54, 60−68

trailing edge driven by dynamic microtubules that target focal adhesions to trigger their disassembly.[20] Thus, dynamic rearrangements in both structural networks are required for malignant cells to move and metastasize. Consequently, critical components of malignant transformation and metastasis include changes in a cell's mechanical phenotype, including elasticity, viscosity, adhesion, and force generation.[22,23]

To begin to explore Syk-dependent changes in the mechanical properties of tumor cells, we examined cells expressing or lacking the kinase using AFM to map the topography and mechanical properties of live cells. Interestingly, we found that the expression of Syk in highly invasive breast carcinoma cells dramatically reduced cell height, increased elasticity, increased viscosity, and allowed visualization of a more substantial microtubule network. Consistent with these observations, the microtubules of Syk-expressing cells were more stable to nocodazole-induced depolymerization and were more highly acetylated than those of Syk-deficient cells. This effect of Syk on microtubule stability, which required protein phosphorylation, was modulated, in part, through the microtubule-associated protein, MAP1B, a major substrate for Syk in MDA-MB-231 tumor cells.[24] Consequently, down modulation of MAP1B levels in cells attenuated the Syk-dependent increase in microtubule stability and reversed much of the effect of Syk expression on the nanomechanical properties of invasive cancer cells.

EXPERIMENTAL PROCEDURES

Cells. MDA-MB-231 and BT549 breast cancer cells were purchased from ATCC. A line of MDA-MB-231 cells expressing Syk-EGFP upon incubation with tetracycline was constructed using the T-REx system (Invitrogen) as described previously.[18] Cells were cultured in Dulbecco's modified Eagle's medium (DMEM) containing 10% FBS, 100 units/mL penicillin, and 100 μg/mL streptomycin. The expression of Syk-EGFP was induced where indicated by the addition of 1 μg/mL doxycycline for 24 h.

Immunofluorescence Microscopy. Cells cultured on coverslips were fixed with cold methanol for 10 min, blocked in PBS containing 10% goat serum and 0.01% Triton X-100, and then stained with antibodies against α-tubulin (T5168, Sigma), acetylated tubulin (T6793, Sigma), MAP1B (4528, Sigma), or c-Src (ab47405, Abcam). Bound primary antibodies were detected using an AlexaFluor 594-conjugated goat anti-mouse IgG secondary antibody (Invitrogen). Coverslips were mounted with ProLong Gold Antifade reagent (Invitrogen) for fluorescence microscopy. Slides were examined by an Olympus BH2-RFCA fluorescence microscope with a 60× objective equipped with a Sony DXC-950 3CCD color camera and Northern Eclipse version 5.0 from Empix Imaging (Mississauga, ON).

Microtubule Stability Assay. MDA-MB-231 or BT549 cells either expressing or lacking Syk-EGFP or transfected to overexpress c-Src were cultured on coverslips and treated with 10 μM nocodazole suspended in DMEM for 30 min. Cells were fixed and stained for α-tubulin. Microtubule stability was assessed by measuring from microscopic images the length of the residual microtubule network extending from the nucleus to the farthest exterior edge of the cell. More than 100 cells of each type were measured for each treatment.

Western Blotting. Cells were lysed in buffer containing 50 mM Tris-HCl (pH 7.4), 150 mM NaCl, 1% NP-40, 0.25% sodium deoxycholate, 1 mM EGTA, 10% glycerol, and protease inhibitor cocktail (65621, AbCam). The lysates were centrifuged at 14000*g* for 1 min. Proteins in the supernatant were separated by sodium dodecyl sulfate−polyacrylamide gel electrophoresis (SDS−PAGE) and analyzed by immunoblotting with antibodies against Syk (N19, Santa Cruz), acetylated tubulin (T6793, Sigma), acetylated lysine (9441, Cell Signaling Technologies), or MAP1B (N-19, Santa Cruz).

Transfection and shRNA Experiments. A stable line of Tet-inducible MDA-MB-231 cells with reduced levels of MAP1B was generated starting with a set of five TRC small hairpin RNAs (shRNA) individually packaged into lentiviral particles (Thermo Scientific). Cells were plated in 10 cm plates at approximately 70% confluence and infected with each shRNA-expressing lentivirus according to the manufacturer's protocol. Cells containing integrated lentiviral sequences were selected using puromycin (1 μg/mL). Medium containing puromycin was replaced every 2 days until resistant colonies were observed. Knockdown of MAP1B was confirmed by immunofluorescence and Western blotting using antibodies against MAP1B. MDA-MB-231 cells were transiently transfected with expression plasmids encoding Syk-EGFP or c-Src (Addgene plasmid 13663) using lipofectamine 2000.

Atomic Force Microscopy Experiments. A MFP3D-Bio (Asylum Research) atomic force microscope mounted on an Olympus IX71 inverted optical microscope inside an acoustically isolated enclosure was used. Standard soft biolevers (BL-TR400PB, Olympus) with a nominal spring constant of 0.09 N/m, nominal tip half-angle of 35°, and nominal radius of 42 ± 12 nm were used for imaging and measurements. For cantilever calibration, an atomically flat and stiff mica substrate with culture medium was used to determine a force−distance curve to calculate the photodetector sensitivity value. The spring constant was obtained by using the thermal noise method.[25] The typical estimated values for the effective cantilever spring constant were in the range of 0.06−0.1 N/m and Q factors in the range of 1.6−2. Prior to AFM experiments, cancer cells were plated on gelatin-coated fluorodish cell culture dishes (WPI, FL) and grown with culture medium for a period of 1−2 days in an incubator at 37 °C and 5% CO_2. Where indicated, the expression of Syk-EGFP was induced. Cancer cells were then transferred and mounted on the AFM XY scanner for the experimental procedure. Two different AFM modes were used in this study. For quantitative high-spatial resolution images of cancer cells, an adaptation of AM-AFM known as multiharmonic AFM was used.[1,26,27] The iDrive (Asylum Research) AC mode was used for these experiments, which uses Lorentz force excitation to directly oscillate the AFM probe near the resonance frequency of its first frequency flexural mode (typically 7−8.5 kHz). We used the multiharmonic AFM theory as described previously[1] to calculate the local nanomechanical properties, specifically the stiffness and damping of a local Kelvin−Voigt element. The multiharmonic AFM experiments were performed under near-physiological conditions in PBS at 37 °C. To measure the Young's modulus of cancer cells, the force−volume ($F-V$) mode was used, yielding 32 pixel × 32 pixel images with an approximate time of 35 min per image.[28] The relative trigger used for these experiments was to adjust the cantilever loading force to 1.5 nN to minimize the damage to the cells. The Sneddon's contact mechanics model, which is a modification of the standard Hertz contact mechanics model for conical tips, was used to fit all of the recorded force−distance ($F-Z$)

dx.doi.org/10.1021/bi500325n | *Biochemistry* 2015, 54, 60−68

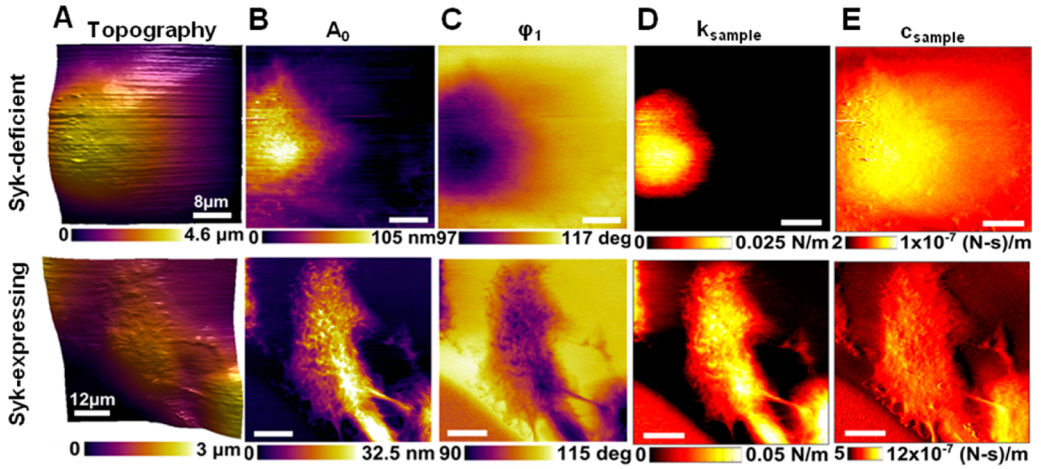

Figure 1. High-resolution (256 pixels × 256 pixels) AM-AFM images showing nanoscale changes of material compositional contrast resulting from the expression of Syk. (A) Topography images of live MDA-MB-231 cells lacking Syk (top panel) or induced to express Syk-EGFP (bottom panel). (B and C) AM-AFM compositional contrast images of mean cantilever deflection A_0 and phase lag (ϕ_1) showing subcellular feature details. (D and E) Maps of local nanomechanical properties, dynamic stiffness k_{sample}, and damping c_{sample} of a local Kelvin–Voigt element extracted using multiharmonic theory.

curves.[29,30] The Sneddon model for a cone-shaped AFM tip used in this study

$$F_{ts} = \frac{2}{\pi}\frac{E}{1-\nu_s^2}\tan(\theta)\delta^2$$

where F_{ts} is the tip–sample interaction force (newtons), E elastic Young's modulus (pascals), ν_s Poisson's ratio of 0.5 for soft samples, θ the half-space cone angle of the cantilever, and δ the sample mean indentation.[30] The main assumptions in this model are that (a) the tip can be modeled as a rigid conical indenter, (b) the cell can be modeled as an elastic half-space with a well-defined boundary, and (c) the tip indentation is much smaller than the cell thickness. The first assumption is widely made even when pyramidal tips are used, as in this case; however, it is known that this assumption leads to small errors in the estimation of Young's modulus.[31] The second assumption has been called into question because AFM elasticity measurements on cells are affected by artifacts from the brushlike structure and the large stiffness of the underneath substrate.[32] This effect is particularly strong for AFM probes with microspheres attached at the end.[33] Thus, in this work, we used a sharp tip that significantly reduces the number of interactions with the brushlike layer, allowing the direct use of Sneddon's contact mechanics model. The third assumption is usually violated when the tip indentation exceeds 10–20% of the cell thickness.[34] In this case, a multiplicative correction of Sneddon's model has been proposed by Gavara and Chadwick,[35] named BECC, which corrects for the bottom effect for conical AFM tips. For a cell thickness of ~4 μm as used in this work, an indentation of more than 400–800 nm would be needed to violate the assumptions of the standard Sneddon model. However, all the measurements made here have been for indentations of less than 400 nm. This, together with the fact that the coefficients of determination (R_2) of the fits of the Sneddon model to the data are very high, gives us confidence that the model is appropriate to use to quantify these measurements. All AFM force–volume experiments were performed in culture medium at 37 °C, while multiharmonic imaging was performed in PBS.

RESULTS

Multiharmonic AFM Mapping of Physical Properties of Breast Cancer Cells. Tumor suppressor functions attributed to Syk reflect its ability to inhibit motility and metastasis when re-expressed in highly invasive cancer cells.[10,18] Because the molecular mechanisms underlying this property are poorly understood, we examined how the expression of Syk would affect the physical properties of an invasive breast cancer cell line. MDA-MB-231 cells have a mesenchymal phenotype, are highly motile, and readily form metastases upon being introduced into mice.[36] The expression of exogenous Syk in metastatic breast cancer cells inhibits their motility and markedly attenuates the formation of distant metastases.[10] We generated a stable line of MDA-MB-231 cells in which the expression of Syk with a C-terminally enhanced green fluorescent protein tag (Syk-EGFP) was under the control of a tetracycline-inducible promoter.[18] These cells lack endogenous Syk but, upon being treated with tetracycline, express Syk-EGFP.

As shown previously, the expression of Syk-EGFP in MDA-MB-231 cells markedly attenuates their motility.[18] To begin to explore possible mechanisms by which Syk influences the properties of MDA-MB-231 cells, we used multiharmonic AFM to image at high spatiotemporal resolution live cells either lacking Syk or induced to express Syk-EGFP. In multiharmonic AFM, a microcantilever is excited near the natural first flexural frequency, pressed down against the cell, and scanned across the cell to collect the resulting changes in the vibration harmonic content, which represents changes in nanomechanical physical properties of the cells.[1] The topography and nanoscale compositional contrast images [mean cantilever deflection or the zeroth harmonic (A_0) and first harmonic phase lag (ϕ_1)] for a typical pair of cells are illustrated in Figure 1. Second harmonics were not observed on these cells. The compositional contrast images of cells lacking Syk (Figure 1A–C) exhibit very few cellular features and no well-defined cytoskeletal organization consistent with the nature of these cells, which are highly motile with a dynamic internal cytoskeleton. These cells exhibited a rounded phenotype and were often removed easily from the gelatin-coated dish during scanning likely

dx.doi.org/10.1021/bi500325n | Biochemistry 2015, 54, 60–68

because of their high level of motility and decreased strength of adhesion. In contrast, the cells expressing Syk-EGFP were characterized by an increased level of cell spreading (decreased cell height) and a more organized subsurface cytoskeletal structure (Figure 1, bottom panels). Syk-EGFP-expressing cells also were less likely to evade the cantilever, because of decreased motility and increased adhesion. The measured compositional contrast images A_0 and ϕ_1 were combined to extract the local nanomechanical properties, specifically the stiffness and damping of local Kelvin−Voigt element k_{sample} and c_{sample}. k_{sample} is a measurement of the differences in stiffness or rigidity within the cell, and c_{sample} illustrates differences in the damping or cell viscosity (Figure 1; a second example is illustrated in Figure S1 of the Supporting Information).[1,27] The induction of Syk-EGFP expression in MDA-MB-231 cells dramatically increased both cell stiffness and viscosity.

Effects of Syk on Microtubule Stability. The actin and microtubule cytoskeletons provide the intracellular networks that determine many of the physical properties of cells.[37,38] AFM compositional contrast images of cells expressing Syk-EGFP revealed subcellular structures consistent with that of a cytoskeletal network (Figure 1, bottom panels). The size and morphology of this network were more consistent with those of microtubules than those of actin microfilaments when compared to images of cells stained with antibodies against α-tubulin or labeled with rhodamine-phalloidin (Figure S2 of the Supporting Information). F-Actin staining was observed primary at the cell cortex, while microtubule polymers were found throughout the cytoplasm and resembled the cytoskeletal features revealed by AFM.

To study in more detail possible effects of Syk on microtubules, we examined the stability of the microtubule network. MDA-MB-231 cells either lacking or expressing Syk-EGFP were treated with low concentrations of nocodazole for 30 min to promote microtubule depolymerization. It has been shown that differences in the stability of the microtubule network manifest themselves as changes in resistance to nocodazole-induced depolymerization.[39] Cells were fixed and stained with an antibody against α-tubulin and examined by fluorescence microscopy. There was a pronounced difference in the morphology of the nocodazole-treated cells between those lacking Syk, in which the microtubule network was largely disassembled, and those expressing Syk-EGFP, in which cells retained microtubule structures resistant to drug-induced depolymerization (Figure 2A). To quantify these differences, we determined the persistence of the microtubule network by measuring the distance of α-tubulin staining from the nucleus to the perimeter of each cell. Results from a comparison of more than 200 cells are shown in Figure 2B. Nocodazole-treated cells expressing Syk-EGFP exhibited a much greater level of retention of α-tubulin-containing polymers than did cells lacking Syk. In contrast to the expression of Syk, the overexpression of c-Src, which typically enhances cell motility,[40] failed to prevent cells from rounding up following treatment with nocodazole (Figure S3 of the Supporting Information).

Because MDA-MB-231 cells are somewhat unique among breast cancer cell lines in that they express activated K-Ras, we also examined the effects of Syk expression in BT549 human breast carcinoma cells, which do not express activated K-Ras and also lack endogenous Syk.[10] Again, the expression in these cells of Syk stabilized the microtubule networks and inhibited the rounding up of cells in response to nocodazole, similar to the results observed for MDA-MB-231 cells (Figure S4 of the Supporting Information).

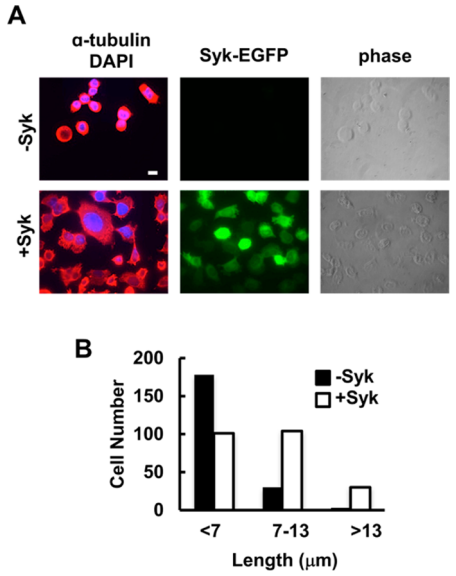

Figure 2. Stabilization of microtubules through the expression of Syk. (A) MDA-MB-231 cells lacking Syk (−Syk) or expressing Syk (+Syk) and treated with nocodazole were stained with an antibody against α-tubulin and a fluorescently tagged secondary antibody, and with DAPI to mark the nucleus. Cells were examined by phase contrast and fluorescence microscopy to detect α-tubulin (red), nuclei (blue), and Syk-EGFP (green). (B) Distances from the cell nucleus to the cell boundary as marked by α-tubulin fluorescence. Cells were grouped into three categories as indicated. The bar is 10 μm.

A hallmark of stable microtubules is an increase in their extent of acetylation on lysine.[41] Consequently, we asked if tubulin from Syk-EGFP-expressing cells was more highly acetylated than tubulin from cells lacking Syk. MDA-MB-231 cells either not induced or induced to express Syk-EGFP (Figure 3A) were lysed in microtubule stabilizing buffer containing 1% NP-40 and separated by centrifugation into soluble (monomer) and insoluble (polymer) fractions. Proteins in each fraction were separated by SDS−PAGE and analyzed by Western blotting using an antibody that recognizes lysine-acetylated α-tubulin. Acetylated tubulin was found predominantly in the polymer fraction as expected (Figure 3B). Tubulin from Syk-EGFP-expressing cells contained an approximately 3-fold higher level of acetylated lysine, consistent with the increased stability of the microtubule network in these cells. An increase in the level of highly acetylated microtubules in the Syk-EGFP-expressing cells was confirmed by immunofluorescence microscopy (Figure 3C). When treated with nocodazole, the Syk-EGFP-expressing cells also retained more lysine-acetylated microtubule polymers than cells lacking Syk-EGFP. Similar results were observed in MDA-MB-231 cells transiently transfected to express Syk-EGFP as compared to Syk-deficient cells (Figure S5 of the Supporting Information).

Role of Phosphorylation in the Stabilization of Microtubules. To determine if Syk-dependent protein phosphorylation was involved in modulating cytoskeletal dynamics, we asked if the catalytic activity of Syk was required for the promotion of microtubule stability. We generated a line of MDA-MB-231 cells in which the expression of a catalytically inactive version of Syk-EGFP [Syk-EGFP(K396R)] was under the control of a tetracycline-inducible promoter. Cells induced

dx.doi.org/10.1021/bi500325n | Biochemistry 2015, 54, 60−68

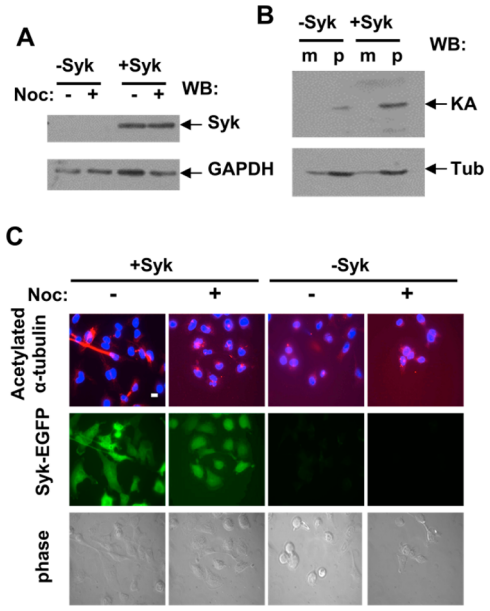

Figure 3. Syk expression increases the levels of acetylated tubulin. (A) Western blot analysis of Syk expression in MDA-MB-231 cells lacking Syk (−Syk) or induced to express Syk-EGFP (+Syk). GAPDH was detected as a loading control. (B) Lysates of MDA-MB-231 cells lacking Syk (−Syk) or induced to express Syk (+Syk) were separated into soluble and insoluble fractions to separate α-tubulin/β-tubulin monomers (m) from tubulin polymers (p). Lysine-acetylated tubulin (KA) and α-tubulin (Tub) were detected by Western blotting. (C) MDA-MB-231 cells lacking Syk (−Syk) or expressing Syk-EGFP (+Syk) and treated without (−) or with (+) nocodazole were stained with an antibody against acetylated α-tubulin and a fluorescently tagged secondary antibody, and with DAPI to mark the nucleus. Cells were examined by phase contrast (bottom panels) and fluorescence microscopy to detect α-tubulin (red) and nuclei (blue) (top panels) and Syk-EGFP (green) (middle panels). The bar is 10 μm.

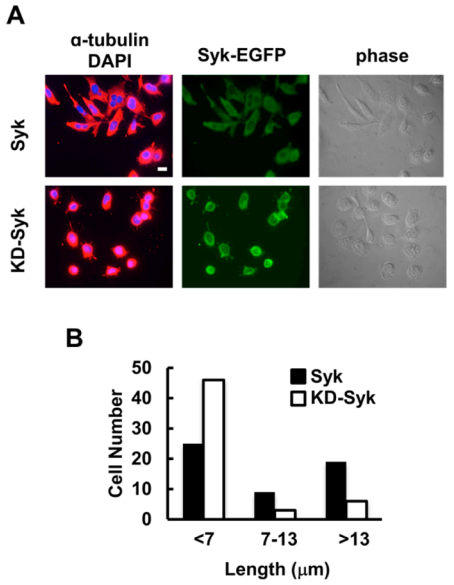

Figure 4. Stabilization of microtubules requires the catalytic activity of Syk. (A) MDA-MB-231 cells expressing Syk-EGFP (Syk) or Syk-EGFP(K396R) (KD-Syk) and treated with nocodazole were stained with an antibody against α-tubulin and a fluorescently tagged secondary antibody, and with DAPI to mark the nucleus. Cells were examined by phase contrast and fluorescence microscopy to detect α-tubulin (red), nuclei (blue), and Syk-EGFP (green). (B) Distances from the cell nucleus to the cell boundary as marked by α-tubulin fluorescence. Cells were grouped into three categories as indicated. The bar is 10 μm.

to express Syk-EGFP or Syk-EGFP(K396R) were treated with nocodazole (10 μM) for 30 min, fixed, immunostained with an α-tubulin antibody, and examined under the fluorescence microscope. There was an obvious difference in the morphology of drug-treated cells expressing active versus inactive kinase (Figure 4). As compared to cells expressing Syk-EGFP, Syk-EGFP(K396R)-expressing cells were more rounded because of microtubule depolymerization and resembled cells that lacked Syk. Thus, the ability of Syk to stabilize microtubules was a function of its catalytic activity.

Identification of a Syk Substrate Involved in Microtubule Stability. To investigate how active Syk might promote microtubule stability, we searched for proteins from MDA-MB-231 cells that were both phosphorylated on tyrosine in a manner dependent on the exogenous expression of Syk and involved in the stabilization of microtubules. The results of this large-scale phosphoproteomic analysis of Syk-dependent phosphorylated substrates were published recently.[24]

Among the Syk-dependent phosphoproteins identified in our study was MAP1B, a microtubule-associated protein known to enhance microtubule stability.[41−43] We identified 17 distinct sites of tyrosine phosphorylation on MAP1B isolated from MDA-MB-231 cells expressing exogenous Syk that were not phosphorylated in cells lacking the kinase.[24] Ten of these sites (and an additional six) were also phosphorylated on MAP1B isolated from DG75 B lymphoma cells, which are cells that express endogenous Syk at normal levels. Multiple MAP1B-derived phosphopeptides were also identified when tyrosine-phosphorylated tryptic peptides from MDA-MB-231 or DG75 cells were isolated, dephosphorylated *in vitro*, and then rephosphorylated by recombinant Syk.[44] Many of these sites are clustered within an area of MAP1B known as the imperfect repeat region (Table SI of the Supporting Information).[45,46]

Effect of the Depletion of MAP1B on Microtubule Stability. To determine if MAP1B was critically involved in microtubule stabilization in MDA-MB-231 cells, we reduced the level of the protein through RNA interference. A collection of five different lentiviruses were used individually to deliver small hairpin RNAs (shRNAs) targeting MAP1B to MDA-MB-231 cells either expressing or lacking Syk-EGFP. Two of the five shRNAs successfully reduced the level of MAP1B as measured by the immunofluorescence of infected and antibiotic-selected cells (an example of one of these is illustrated in Figure 5A) or by Western blotting (Figure 5C). To ascertain a role for MAP1B in Syk-dependent microtubule stability, we induced the expression of Syk-EGFP in MDA-MB-231 cells expressing normal or reduced levels of MAP1B. Cells were treated with nocodazole (10 μM) for 30 min, fixed, and immunostained using an antibody against α-tubulin (Figure 5B). The size of the drug-resistant microtubule cytoskeleton was then measured (Figure 5C). Despite the expression of Syk-EGFP, the MAP1B knockdown cells displayed a morphology similar to that of cells lacking Syk as cells were more rounded and failed to retain stable microtubule networks.

Influence of MAP1B on the Physical Properties of MDA-MB-231 Cells. To investigate roles for Syk in conjunction with MAP1B in modulating the physical properties of cancer cells, we measured the influence of Syk on the topography and elasticity of MDA-MB-231 cancer cells in the

dx.doi.org/10.1021/bi500325n | *Biochemistry* 2015, 54, 60−68

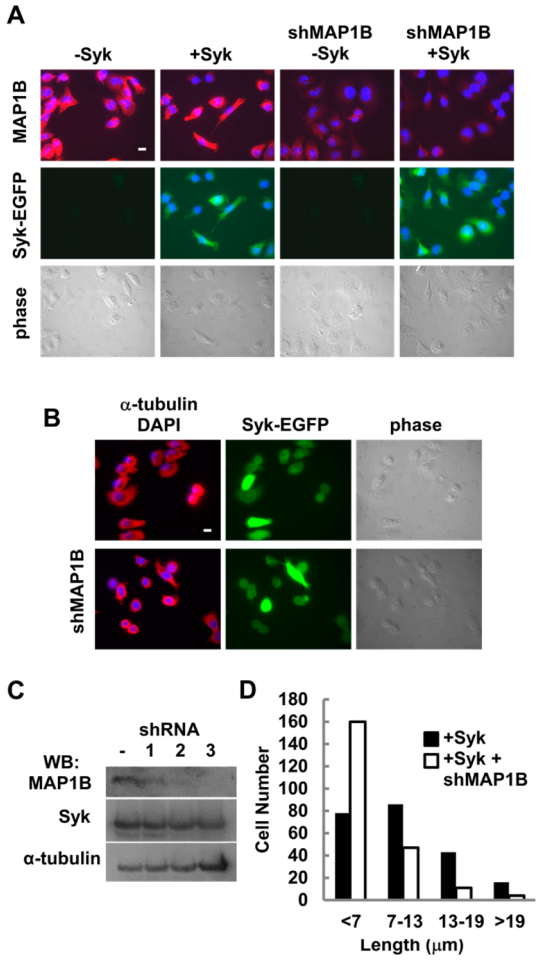

Figure 5. Syk-dependent stabilization of microtubules is attenuated by the loss of MAP1B. (A) MDA-MB-231 cells were treated (shMAP1B) or were not treated with a lentivirus expressing a short hairpin RNA directed against the MAP1B mRNA. Cells were not induced (−Syk) or induced (+Syk) to express Syk-EGFP. Cells were stained with an antibody against MAP1B and a fluorescently tagged secondary antibody, and with DAPI to mark the nucleus. Cells were examined by phase contrast (bottom panels) and fluorescence microscopy to detect MAP1B (red), nuclei (blue), and Syk-EGFP (green). (B) MDA-MB-231 cells without or with knockdown of MAP1B (shMAP1B), induced to express Syk-EGFP, and treated with nocodazole were stained with an antibody against α-tubulin and a fluorescently tagged secondary antibody, and with DAPI to mark the nucleus. Cells were examined by phase contrast and fluorescence microscopy to detect α-tubulin (red), nuclei (blue), and Syk-EGFP (green). (C) MDA-MB-231 cells without (−) or with knockdown of MAP1B with one of three example shRNAs and induced to express Syk-EGFP were analyzed by Western blotting for the presence of MAP1B, Syk-EGFP (Syk), or α-tubulin. (D) Lengths of residual microtubules measured from the cell nucleus to the cell boundary. Cells were grouped into four categories as indicated. The bar is 10 μm.

presence or absence of normal levels of MAP1B. We estimated elasticity values by AFM using the force−volume (F−V) mode to compare changes in the relative elastic modulus. In F−V imaging, the AFM probe approaches, is pushed against, and is retracted from the cell surface on a grid of points predefined by the user to record a resulting force−distance curve. Subsequently, the images are processed offline to extract two quantities of interest: cell height and elasticity.

Examples of the topography and elasticity measurements of cells lacking Syk, induced to express Syk-EGFP, or induced to express Syk-EGFP and lacking MAP1B are shown in Figure 6A.

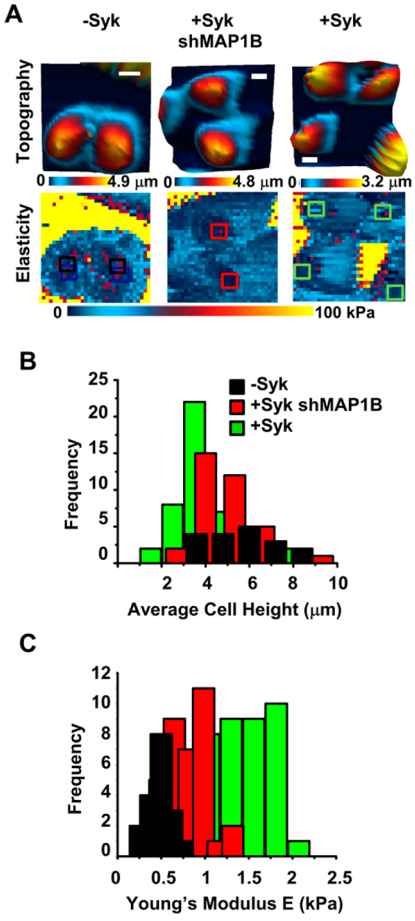

Figure 6. Knockdown of MAP1B attenuates the Syk-dependent changes in the cellular phenotype. (A) Topographic images and elasticity maps of MDA-MB-231 cells lacking Syk (−Syk) or expressing Syk (+Syk) without or with shRNA directed against MAP1B (shMAP1B) were acquired by AFM using force−volume mode. On the elasticity maps are insets (squares) marking the locations of 3 pixels × 3 pixels extracted to analyze the resulting cell height and elasticity. Images were taken at a trigger force of 2 nN (32 pixels × 32 pixels). The bar is 10 μm. (B) Histogram illustrating the distribution of heights for 45 MDA-MB-231 cells either lacking Syk (−Syk) or expressing Syk (+Syk) without or with shRNA directed against MAP1B (shMAP1B). (C) Histogram illustrating the distribution of elasticities for 45 MDA-MB-231 cells either lacking Syk (−Syk) or expressing Syk (+Syk) without or with shRNA directed against MAP1B (shMAP1B).

A second example is shown in Figure S6 of the Supporting Information. The respective topography maps are shown in the top panels and elasticity maps in the bottom panels. The comparative maximal cell height and elasticity histograms in the nuclear region from multiple cells are illustrated in panels B and C of Figure 6, respectively. The induction of Syk-EGFP expression in MDA-MB-231 cells dramatically decreased the height of the average cell from 5.62 ± 1.58 to 3.83 ± 1.26 μm. The cell height was increased to 4.87 ± 1.22 μm by decreasing the intracellular level of MAP1B in the Syk-EGFP-expressing cells. Similarly, the expression of Syk-EGFP increased the cellular elasticity from 0.488 ± 0.199 to 1.35 ± 0.387 kPa.

dx.doi.org/10.1021/bi500325n | *Biochemistry* 2015, 54, 60−68

Again, the knockdown of MAP1B partially reversed this effect, reducing the elasticity of Syk-expressing cells to 0.812 ± 0.224 kPa.

These results indicate that the expression of Syk has pronounced effects on the physical properties of MDA-MB-231 cells (decreased height and increased stiffness) and that these are mediated in part, but not in full, by the phosphorylation of MAP1B. Thus, many of the changes in the physical properties of MDA-MB-231 cells resulting from the expression of Syk are mediated by alterations in the microtubule cytoskeleton.

DISCUSSION

To disseminate from the site of a primary tumor, a cancer cell of epithelial origin must detach from neighboring cells, migrate from the tumor site, extravasate into either the vascular or lymphatic systems, travel to a distant site, extravasate from the circulation, and establish through cell division a new tumor mass.[3,4,47] To accomplish this, transformed epithelial cells undergo EMT, whereby they lose E-cadherin-mediated contacts, develop strong cell−extracellular matrix adhesions, and undergo cytoskeletal rearrangements that allow them to achieve enhanced migratory and invasive properties.[48] Considerable work has been done using AFM to measure variations in mechanical properties as a function of metastatic potential, allowing the detection of tumor progression. The resulting changes in the mechanical properties of tumor cells that accompany EMT as measured by AFM include decreased stiffness, consistent with many observations that cancer cells exhibit an elasticity significantly decreased in comparison to those of their normal counterparts.[38,49] Prior work has shown that metastatic cancer cells are more than 70% softer than benign cells.[50] A decrease in the Young's moduli has been reported for prostate cancer cells with increasing metastatic potential.[51] The inhibition or knockdown of Syk in breast epithelial cells or Ras-dependent pancreatic carcinomas induces phenotypic changes characteristic of EMT.[5,6] Consistent with these observations, the re-expression of Syk in highly invasive MDA-MB-231 cells, which have a mesenchymal phenotype, substantially decreases cellular elasticity and increases viscosity and the level of adhesion.

The intrinsic stiffness of cells is a property of cellular cytoskeletal networks including microtubules and actin microfilaments. The appearance of subcellular structures resembling microtubules revealed by AFM selectively in Syk-expressing cells prompted us to explore the effects of the kinase on tubulin polymers. Microtubules were more stable in Syk-expressing cells as measured by their insensitivity to drug-induced depolymerization and an increased content of acetylated lysine, which is a marker of more stable microtubules. Several studies have demonstrated interactions between Syk and microtubules or proteins involved in the regulation of microtubule organization. Syk can bind to and phosphorylate tubulin, and a fraction of the kinase localizes to centrosomes and associates with a number of centrosomal proteins.[44,52,53] The movement of Syk to the centrosome is dependent on both the catalytic activity of Syk and its movement along microtubules mediated by the dynein−dynactin complex.[54] A phosphoproteomic analysis of Syk-dependent substrates identified several centrosomal and microtubule-associated proteins.[24,44] The substrate with the most identified sites of phosphorylation was MAP1B, a microtubule-associated protein found most prominently in the nervous system.[55] The expression of MAP1B in MDA-MB-231 cells was unexpected. However, the abnormal expression of tissue differentiation markers has been noted previously in many cancer cells, including MDA-MB-231 and other breast cancer cells.[56] We also detected the phosphorylation of MAP1B on multiple tyrosines in DG75 cells, an EBV-transformed human B cell lymphoma cell line unrelated to MDA-MB-231.[24] On the basis of the PhosphoSitePlus database, phosphotyrosine-containing peptides derived from MAP1B also have been identified in a variety of tumor cell types, including bladder, colorectal, non-small lung, esophageal, Hodgkins lymphoma, and chronic myelogenous leukemia.[57]

MAP1B is developmentally regulated in the nervous system where it plays an important role in neurite and axon extension through its ability to bind to dynamic microtubules in growth cones.[43,58−60] The exogenous expression of MAP1B in non-neuronal cells stabilizes microtubules to drug-induced depolymerization and increases the abundance of acetylated microtubules.[41,61] When present in MDA-MB-231 cells, these activities of MAP1B are enhanced considerably by the co-expression of Syk, which phosphorylates the protein on multiple tyrosines. MAP1B has previously been shown to be extensively phosphorylated by serine/threonine kinases on a variety of sites spread out throughout the central region of the molecule.[62] Phosphorylation has been shown to modulate the ability of the protein to bind to and stabilize microtubules depending on the site or sites that are modified.[62] The sites phosphorylated by Syk are largely clustered within the hydrophilic imperfect repeat region of MAP1B, a region not directly involved in binding microtubules.[46] This region contains multiple consensus sites of serine phosphorylation for casein kinase 2 (CK2), which phosphorylates MAP1B and enhances its binding to microtubules.[63,64] It is reasonable to predict that the phosphorylation of MAP1B by Syk within this same acidic region would also enhance MAP1B−microtubule interactions, accounting for the ability of Syk to promote microtubule stability. Interestingly, three of these sites are found within pYXXL/I motifs, which are sequences recognized by a subset of SH2 domain-containing proteins, including Syk itself. Such an interaction may help explain the abundance of tyrosines on MAP1B that become phosphorylated in cells expressing both MAP1B and Syk. Because dynamic microtubules play major roles in motility by modulating the disassembly of focal adhesions and retraction of the trailing edge of migrating cells, increased stability conferred by the enhanced binding of phosphorylated MAP1B could reasonably account for many aspects of Syk's ability to limit the motility of highly invasive cancer cells. It is interesting that modulation of the activity of a microtubule-stabilizing factor produces such dramatic changes in the mechanical properties of cancer cells as changes in the stiffness of cells are most often attributed to alterations in the actin cytoskeleton.[38,65,66] However, there is considerable cross-talk between cytoskeletal systems. For example, Rho family GTPases, which control actin dynamics, are, in turn, regulated by dynamic microtubules that interact in a polymerization-dependent fashion with Rho guanine nucleotide exchange factor 190RhoGEF.[67] Thus, dynamic microtubules are major modulators of the mechanical properties that affect fundamental processes such as cell adhesion and motility.

dx.doi.org/10.1021/bi500325n | Biochemistry 2015, 54, 60−68

■ ASSOCIATED CONTENT

Supporting Information

A high-resolution AM-AFM image of material composition maps of cells expressing Syk-EGFP, fluorescence staining of microtubule and actin microfilament networks of MDA-MB-231 cells, a comparison of MDA-MB-231 cells overexpressing either Syk-EGFP or c-Src, the effect of Syk-EGFP expression on the stability of microtubules in BT549 cells for nocodazole treatment, a close-up image of nocodazole-stable acetylated microtubules in MDA-MB-231 cells lacking or expressing Syk-EGFP, and topographic images and elasticity maps of MDA-MB-231 cells without or with knockdown of MAP1B. This material is available free of charge via the Internet at http://pubs.acs.org.

■ AUTHOR INFORMATION

Corresponding Authors

*E-mail: raman@purdue.edu. Phone: (765) 494-5733.
*E-mail: geahlen@purdue.edu. Phone: (765) 494-1457.

Author Contributions

M.O.K. and A.C. contributed equally to this work.

Funding

This research was supported in part by National Institutes of Health Grants AI098132 and CA115465 (R.L.G.) and Grant DMR-1008189 from the National Science Foundation Materials World Network (A.R.). M.O.K. was supported by National Science Foundation Graduate Research Fellowship DGE-0833366. The DNA sequencing facility was supported by National Cancer Institute CCSG CA23168 to the Purdue University Center for Cancer Research.

Notes

The authors declare no competing financial interests.

■ REFERENCES

(1) Raman, A., Trigueros, S., Cartagena, A., Stevenson, A. P. Z., Susilo, M., Nauman, E., and Contera, S. A. (2011) Mapping nanomechanical properties of live cells using multi-harmonic atomic force microscopy. *Nat. Nanotechnol. 6*, 809−814.

(2) Yilmaz, M., and Christofori, G. (2009) EMT, the cytoskeleton, and cancer cell invasion. *Cancer Metastasis Rev. 28*, 15−33.

(3) Thiery, J. P. (2002) Epithelial-mesenchymal transitions in tumour progression. *Nat. Rev. Cancer 2*, 442−454.

(4) Yang, J., and Weinberg, R. A. (2008) Epithelial-mesenchymal transition: At the crossroads of development and tumor metastasis. *Dev. Cell 14*, 818−829.

(5) Singh, A., Greninger, P., Rhodes, D., Koopman, L., Violette, S., Bardeesy, N., and Settleman, J. (2009) A gene expression signature associated with "K-Ras addiction" reveals regulators of EMT and tumor cell survival. *Cancer Cell 15*, 489−500.

(6) Sung, Y. M., Xu, X., Sun, J., Mueller, D., Sentissi, K., Johnson, P., Urbach, E., Seillier-Moiseiwitsch, F., Johnson, M. D., and Mueller, S. C. (2009) Tumor suppressor function of Syk in human MCF10a in vitro and normal mouse mammary epithelium in vivo. *PLoS One 4* (10), e7445.

(7) Geahlen, R. L. (2009) Syk and pTyr'd: Signaling through the B cell antigen receptor. *Biochim. Biophys. Acta 1793*, 1115−1127.

(8) Mócsai, A., Ruland, J., and Tybulewicz, V. L. (2010) The SYK tyrosine kinase: A crucial player in diverse biological functions. *Nat. Rev. Immunol. 10*, 387−402.

(9) Zhang, J., Benavente, C. A., McEvoy, J., Flores-Otero, J., Ding, L., Chen, X., Ulyanov, A., Wu, G., Wilson, M., Wang, J., Brennan, R., Rusch, M., Manning, A. L., Ma, J., Easton, J., Shurtleff, S., Mullighan, C., Pounds, S., Mukatira, S., Gupta, P., Neale, G., Zhao, D., Lu, C., Fulton, R. S., Fulton, L. L., Hong, X., Dooling, D. J., Ochoa, K., Naeve, C., Dyson, N. J., Mardis, E. R., Bahrami, A., Ellison, D., Wilson, R. K., Downing, J. R., and Dyer, M. A. (2012) A novel retinoblastoma therapy from genomic and epigenetic analyses. *Nature 481*, 329−334.

(10) Coopman, P. J. P., Do, M. T. H., Barth, M., Bowden, E. T., Hayes, A. J., Basyuk, E., Blancato, J. K., Vezza, P. R., McLeskey, S. W., Mangeat, P. H., and Mueller, S. C. (2000) The Syk tyrosine kinase suppresses malignant growth of human breast cancer cells. *Nature 406*, 742−747.

(11) Minobe, K., Onda, M., Iida, A., Kasumi, F., Sakamoto, G., Nakamura, Y., and Emi, M. (1998) Allelic loss on chromosome 9q is associated with lymph node metastasis of primary breast cancer. *Jpn. J. Cancer Res. 89*, 916−922.

(12) Yuan, Y., Mendez, R., Sahin, A., and Dai, J. L. (2001) Hypermethylation leads to silencing of the SYK gene in human breast cancer. *Cancer Res. 61*, 5558−5561.

(13) Moroni, M., Soldatenkov, V., Zhang, L., Zhang, Y., Stoica, G., Gehan, E., Rashidi, B., Singh, B., Ozdemirli, M., and Mueller, S. C. (2004) Progressive loss of Syk and abnormal proliferation in breast cancer cells. *Cancer Res. 64*, 7346−7354.

(14) Hoeller, C., Thallinger, C., Pratscher, B., Bister, M. D., Schicher, N., Loewe, R., Heere-Ress, E., Roka, F., Sexl, V., and Pehamberger, H. (2005) The non-receptor-associated tyrosine kinase Syk is a regulator of metastatic behavior in human melanoma cells. *J. Invest. Dermatol. 124*, 1293−1299.

(15) Yuan, Y., Wang, J., Li, J., Wang, L., Li, M., Yang, Z., Zhang, C., and Dai, J. L. (2006) Frequent epigenetic inactivation of spleen tyrosine kinase gene in human hepatocellular carcinoma. *Clin. Cancer Res. 12*, 6687−6695.

(16) Muthusamy, V., Duraisamy, S., Bradbury, C. M., Hobbs, C., Curley, D. P., Nelson, B., and Bosenberg, M. (2006) Epigenetic silencing of novel tumor suppressors in malignant melanoma. *Cancer Res. 66*, 11187−11193.

(17) Layton, T., Stalens, C., Gunderson, F., Goodison, S., and Silletti, S. (2009) Syk tyrosine kinase acts as a pancreatic adenocarcinoma tumor suppressor by regulating cellular growth and invasion. *Am. J. Pathol. 175*, 2625−2636.

(18) Zhang, X., Shrikhande, U., Alicie, B. M., Zhou, Q., and Geahlen, R. L. (2009) Role of the protein tyrosine kinase Syk in regulating cell-cell adhesion and motility in breast cancer cells. *Mol. Cancer Res. 7*, 634−644.

(19) Wittmann, T., and Waterman-Storer, C. M. (2001) Cell motility: Can Rho GTPases and microtubules point the way? *J. Cell Sci. 114*, 3795−3803.

(20) Kaverina, I., and Straube, A. (2011) Regulation of cell migration by dynamic microtubules. *Semin. Cell Dev. Biol. 22*, 968−974.

(21) Gardel, M. L., Schneider, I. C., Aratyn-Schaus, Y., and Waterman, C. M. (2010) Mechanical integration of actin and adhesion dynamics in cell migration. *Annu. Rev. Cell Dev. Biol. 26*, 315−333.

(22) Kumar, S., and Weaver, V. M. (2009) Mechanics, malignancy, and metastasis: The force journey of a tumor cell. *Cancer Metastasis Rev. 28*, 113−127.

(23) Suresh, S. (2007) Nanomedicine: Elastic clues in cancer detection. *Nat. Nanotechnol. 2*, 748−749.

(24) Iliuk, A. B., Martin, V. A., Alicie, B. M., Geahlen, R. L., and Tao, W. A. (2010) In-depth analyses of kinase-dependent tyrosine phosphoproteomes based on metal ion-functionalized soluble nano-polymers. *Mol. Cell. Proteomics 9*, 2162−2172.

(25) Butt, H. J., and Jaschke, M. (1995) Calculation of thermal noise in atomic force microscopy. *Nanotechnology 6*, 1−7.

(26) Cartagena, A., Hernando-Pérez, M., Carrascosa, J. L., de Pablo, P. J., and Raman, A. (2013) Mapping in vitro local material properties of intact and disrupted virions at high resolution using multi-harmonic atomic force microscopy. *Nanoscale 5*, 4729−4736.

(27) Cartagena, A., and Raman, A. (2014) Local viscoelastic properties of live cells investigated using dynamic and quasi-static atomic force microscopy methods. *Biophys. J. 106*, 1033−1043.

(28) Radmacher, M., Fritz, M., Kacher, C. M., Cleveland, J. P., and Hansma, P. K. (1996) Measuring the viscoelastic properties of human platelets with the atomic force microscope. *Biophys. J. 70*, 556−567.

(29) Sneddon, I. N. (1965) The relation between load and penetration in the axisymmetric boussinesq problem for a punch of arbitrary profile. *Int. J. Eng. Sci. (Oxford, U.K.)* 3, 47−57.
(30) Alcaraz, J., Buscemi, L., Grabulosa, M., Trepat, X., Fabry, B., Farré, R., and Navajas, D. (2003) Microrheology of human lung epithelial cells measured by atomic force microscopy. *Biophys. J. 84*, 2071−2079.
(31) Radmacher, M., Fritz, M., and Hansma, P. K. (1995) Imaging soft samples with the atomic force microscope: Gelatin in water and propanol. *Biophys. J. 69*, 264−270.
(32) Sokolov, I., Dokukin, M. E., and Guz, N. V. (2013) Method for quantitative measurements of the elastic modulus of biological cells in AFM indentation experiments. *Methods 60*, 202−213.
(33) Sokolov, I., Iyer, S., Subba-Rao, V., and Gaikwad, R. M. (2007) Detection of surface brush on biological cells in vitro with atomic force microscopy. *Appl. Phys. Lett. 91*, 023902.
(34) Dimitriadis, E. K., Horkay, F., Maresca, J., Kachar, B., and Chadwick, R. S. (2002) Determination of elastic moduli of thin layers of soft material using the atomic force microscope. *Biophys. J. 82*, 2796−2810.
(35) Gavara, N., and Chadwick, R. S. (2012) Determination of the elastic moduli of thin samples and adherent cells using conical atomic force microscope tips. *Nat. Nanotechnol. 7*, 733−736.
(36) Price, J. E., Polyzos, A., Zhang, R. D., and Daniels, L. M. (1990) Tumorigenicity and metastasis of human breast carcinoma cell lines in nude mice. *Cancer Res. 50*, 717−721.
(37) Pelling, A. E., Dawson, D. W., Carreon, D. M., Christiansen, J. J., Shen, R. R., Teitell, M. A., and Gimzewski, J. K. (2007) Distinct contributions of microtubule subtypes to cell membrane shape and stability. *Nanomedicine 3*, 43−52.
(38) Xu, W., Mezencev, R., Kim, B., Wang, L., McDonald, J., and Sulchek, T. (2012) Cell stiffness is a biomarker of the metastatic potential of ovarian cancer cells. *PLoS One 7* (10), e46609.
(39) Bulinski, J. C., and Gundersen, G. G. (1991) Stabilization and posttranslational modification of microtubules during cellular morphogenesis. *BioEssays 13*, 285−293.
(40) Summy, J. M., and Gallick, G. E. (2003) Src family kinases in tumor progression and metastasis. *Cancer Metastasis Rev. 22*, 337−358.
(41) Takemura, R., Okabe, S., Umeyama, T., Kanai, Y., Cowan, N. J., and Hirokawa, N. (1992) Increased microtubule stability and α tubulin acetylation in cells transfected with microtubule-associated proteins MAP1B, MAP2 or tau. *J. Cell Sci. 103*, 953−964.
(42) Pedrotti, B., and Islam, K. (1995) Microtubule associated protein 1B (MAP1B) promotes efficient tubulin polymerisation in vitro. *FEBS Lett. 371*, 29−31.
(43) Tymanskyj, S. R., Scales, T. M., and Gordon-Weeks, P. R. (2012) MAP1B enhances microtubule assembly rates and axon extension rates in developing neurons. *Mol. Cell. Neurosci. 49*, 110−119.
(44) Xue, L., Wang, W.-H., Iliuk, A., Hu, L., Galan, J. A., Yu, S., Hans, M., Geahlen, R. L., and Tao, W. A. (2012) Sensitive kinase assay linked with phosphoproteomics for identifying direct kinase substrates. *Proc. Natl. Acad. Sci. U.S.A. 109*, 5615−5620.
(45) Noiges, R., Stroissnigg, H., Trancikova, A., Kalny, I., Eichinger, R., and Propst, F. (2006) Heterotypic complex formation between subunits of microtubule-associated proteins 1A and 1B is due to interaction of conserved domains. *Biochim. Biophys. Acta 1763*, 1011−1016.
(46) Noble, M., Lewis, S. A., and Cowan, N. (1989) The microtubule binding domain of the microtubule-associated protein MAP-1B contains a repeated sequence motif unrelated to that of MAP-2 and tau. *J. Cell Biol. 109*, 3367−3376.
(47) Savagner, P. (2010) The epithelial-mesenchymal transition (EMT) phenomenon. *Ann. Oncol. 21*, vii89−vii92.
(48) Tsai, J. H., Donaher, J. L., Murphy, D. A., Chau, S., and Yang, J. (2012) Spatiotemporal regulation of epithelial-mesenchymal transition is essential for squamous cell carcinoma metastasis. *Cancer Cell 22*, 725−736.
(49) Buckley, S. T., Medina, C., Davies, A. M., and Ehrhardt, C. (2012) Cytoskeletal re-arrangement in TGF-β1-induced alveolar epithelial-mesenchymal transition studied by atomic force microscopy and high-content analysis. *Nanomedicine 8*, 355−364.
(50) Cross, S. E., Jin, Y., Rao, J., and Gimzewski, J. K. (2007) Nanomechanical analysis of cells from cancer patients. *Nat. Nanotechnol. 2*, 780−783.
(51) Faria, E. C., Ma, N., Gazi, E., Gardner, P., Brown, M., Clarke, N. W., and Snook, R. D. (2008) Measurement of elastic properties of prostate cancer cells using AFM. *Analyst 133*, 1498−1500.
(52) Zyss, D., Montcourrier, P., Vidal, B., Anguille, C., Mérezègue, F., Sahuquet, A., Mangeat, P. H., and Coopman, P. J. (2005) The Syk tyrosine kinase localizes to the centrosomes and negatively affects mitotic progression. *Cancer Res. 65*, 10872−10880.
(53) Peters, J. D., Furlong, M. T., Asai, D. J., Harrison, M. L., and Geahlen, R. L. (1996) Syk, activated by cross-linking the B-cell antigen receptor, localizes to the cytosol where it interacts with and phosphorylates α-tubulin on tyrosine. *J. Biol. Chem. 271*, 4755−4762.
(54) Fargier, G., Favard, C., Parmeggiani, A., Sahuquet, A., Merezegue, F., Morel, A., Denis, M., Molinari, N., Mangeat, P. H., Coopman, P. J., and Montcourrier, P. (2013) Centrosomal targeting of Syk kinase is controlled by its catalytic activity and depends on microtubules and the dynein motor. *FASEB J. 27*, 109−122.
(55) Olmsted, J. B. (1986) Microtubule-associated proteins. *Annu. Rev. Cell Biol. 2*, 421−457.
(56) Zhang, Q., Fan, H., Shen, J., Hoffman, R. M., and Xing, H. R. (2010) Human breast cancer cell lines co-express neuronal, epithelial, and melanocytic differentiation markers *in vitro* and *in vivo*. *PLoS One 5* (3), e9712.
(57) Hornbeck, P. V., Kornhauser, J. M., Tkachev, S., Zhang, B., Skrzypek, E., Murray, B., Latham, V., and Sullivan, M. (2012) PhosphoSitePlus: A comprehensive resource for investigating the structure and function of experimentally determined post-translational modifications in man and mouse. *Nucleic Acids Res. 40*, D261−D270.
(58) Tucker, R. P., Garner, C. C., and Matus, A. (1989) In situ localization of microtubule-associated protein mRNA in the developing and adult rat brain. *Neuron 2*, 1245−1256.
(59) Gonzalez-Billault, C., Avila, J., and Caceres, A. (2001) Evidence for the role of MAP1B in axon formation. *Mol. Biol. Cell 12*, 2087−2098.
(60) Gordon-Weeks, P. R., and Fischer, I. (2000) MAP1B expression and microtubule stability in growing and regenerating axons. *Microsc. Res. Tech. 48*, 63−74.
(61) Ryan, S. D., Bhanot, K., Ferrier, A., De Repentigny, Y., Chu, A., Blais, A., and Kothary, R. (2012) Microtubule stability, Golgi organization, and transport flux require dystonin-a2−MAP1B interaction. *J. Cell Biol. 196*, 727−742.
(62) Scales, T. M. E., Lin, S., Kraus, M., Goold, R. G., and Gordon-Weeks, P. R. (2009) Nonprimed and DYRK1A-primed GSK3β-phosphorylation sites on MAP1B regulate microtubule dynamics in growing axons. *J. Cell Sci. 122*, 2424−2435.
(63) Díaz-Nido, J., Serrano, L., Méndez, E., and Avila, J. (1988) A casein kinase II-related activity is involved in phosphorylation of microtubule-associated protein MAP1B during neuroblastoma cell differentiation. *J. Cell Biol. 106*, 2057−2065.
(64) Ulloa, L., Díaz-Nido, J., and Avila, J. (1993) Depletion of casein kinase II by antisense oligonucleotide prevents neuritogenesis in neuroblastoma cells. *EMBO J. 12*, 1633−1640.
(65) Stricker, J., Falzone, T., and Gardel, M. L. (2010) Mechanics of the F-actin cytoskeleton. *Journal of Biomechanics 43*, 9−14.
(66) Pollard, T. D., and Cooper, J. A. (2009) Actin, a central player in cell shape and movement. *Science 326*, 1208−1212.
(67) van Horck, F. P., Ahmadian, M. R., Haeusler, L. C., Moolenaar, W. H., and Kranenburg, O. (2001) Characterization of p190RhoGEF, a RhoA-specific guanine nucleotide exchange factor that interacts with microtubules. *J. Biol. Chem. 276*, 4948−4956.